Artabolide, a novel polar auxin transport inhibitor isolated from Artemisia absinthium

doi: 10.1016/j.tet.2013.06.052

Tetrahedron 69 (2013) 7001–7005

Contents lists available at SciVerse ScienceDirect

Tetrahedron

journal homepage: www.elsevier.com/locate/tet

Artabolide, a novel polar auxin transport inhibitor isolated from *Artemisia absinthium*☆

Tsukasa Arai [a], Yuta Toda [b], Kiyotaka Kato [b], Kensuke Miyamoto [c], Tsuyoshi Hasegawa [a], Kosumi Yamada [a], Junichi Ueda [b], Koji Hasegawa [a,d], Tsuyoshi Inoue [e], Hideyuki Shigemori [a,*]

[a] *Graduate School of Life and Environmental Sciences, University of Tsukuba, 1-1-1 Tennodai, Tsukuba, Ibaraki 305-8572, Japan*
[b] *Graduate School of Science, Osaka Prefecture University, 1-1 Gakuen-cho, Naka-ku, Sakai, Osaka 599-8531, Japan*
[c] *Faculty of Liberal Arts and Sciences, Osaka Prefecture University, 1-1 Gakuen-cho, Naka-ku, Sakai, Osaka 599-8531, Japan*
[d] *KNC Laboratories Co, Ltd, Hyogo 651-2271, Japan*
[e] *Division of Applied Chemistry, Graduate School of Engineering, Osaka University, 2-1 Yamadaoka, Suita, Osaka 565-0871, Japan*

ARTICLE INFO

Article history:
Received 4 March 2013
Received in revised form 14 June 2013
Accepted 15 June 2013
Available online 21 June 2013

Keywords:
Artabolide
α-Methylene-γ-lactone
Modified Mosher's method
Polar auxin transport inhibitor
X-ray crystal structure analysis

ABSTRACT

A new sesquiterpene with an α-methylene-γ-lactone moiety, artabolide (**1**), and three known derivatives **2**–**4** were isolated from *Artemisia absinthium*. The structure of **1** was elucidated by 1D and 2D NMR analyses, and the absolute configuration was determined using the modified Mosher's method and X-ray crystal structural analysis. Approximately 2.5 μg/plant treatment of artabolide (**1**) exhibited ca. 50% inhibition of polar auxin transport in radish hypocotyls, while **2**–**4** showed no significant inhibitory activity. Therefore, these results support the importance of the α-methylene-γ-lactone moiety for the inhibition of polar auxin transport.

1. Introduction

The plant hormone auxin (indole-3-acetic acid; IAA) plays an important role in plant growth and development. First, IAA is synthesized in the apical part of the shoot and young leaf and is then transported basipetally in a cell-to-cell system. This system, named polar auxin transport, is regulated by the influx carriers AUXIN RESISTANT1/LIKE AUXIN RESISTANT (AUX1/LAX) and efflux carriers PIN-FORMED (PIN) and ATP-binding cassette subfamily B (ABCB) located on the plasma membrane.[1–3]

Over many decades, the mechanism of polar auxin transport has been revealed using synthetic polar auxin transport inhibitors, such as *N*-(1-naphthyl)phthalamic acid (NPA), 2,3,5-triiodobenzoic acid, 9-hydroxyfluorene-9-carboxylic acid, and morphactin. NPA, the most frequently used inhibitor of auxin efflux, has been shown to noncompetitively inhibit PIN and ABCB auxin efflux activities.[4]

Furthermore, a number of flavonoids have been reported to be some of the few naturally occurring inhibitors of polar auxin transport.[5] Flavonoids have also been shown to displace NPA from the plasma membrane binding site.[6] However, except in the case of flavonoids, few studies on natural polar auxin transport inhibitors have been reported.

In our exploratory study of naturally occurring inhibitors of polar auxin transport, we isolated and identified physiologically 4-hydroxy-β-thujone and dehydrocostus lactone as naturally occurring inhibitors of polar auxin transport from some Asteraceae plants.[7] We recently found that the EtOAc-soluble portion of an acetone extract of *Artemisia absinthium* has potent inhibitory activity against polar auxin transport. We successfully isolated a new germacranolide-type sesquiterpene, artabolide (**1**), as the bioactive substance, and also isolated three known pelenolides **2**–**4**. Here we report the isolation, structural elucidation, and the structure–activity relationship of **1**–**4** for polar auxin transport activity.

* Corresponding author. Tel./fax: +81 029 853 4603; e-mail address: shigemori.hideyuk.fn@u.tsukuba.ac.jp (H. Shigemori).

0040-4020/$ – see front matter © 2013 The Authors. Published by Elsevier Ltd. All rights reserved.
http://dx.doi.org/10.1016/j.tet.2013.06.052

2. Result and discussion

2.1. Extraction and separation of *A. absinthium*

The aerial parts of *A. absinthium* (750 gFW) were extracted with 80% acetone/H_2O. The crude extract was partitioned between EtOAc and H_2O. The EtOAc-soluble portion was subjected to repeated silica-gel column chromatography on a Sep-Pak ODS cartridge to afford a mixture of compounds **1** and **2**. The mixture was purified by reversed-phase high-performance liquid chromatography (HPLC) to yield artabolide (**1**, 0.00025%) and hydroxypelenolide (**2**, 0.0022%). The other two fractions shown as brown spots on thin-layer chromatography (TLC) visualized by 10% H_2SO_4/H_2O and heat treatment were subjected to Sep-Pak ODS cartridges and subsequently purified by reversed-phase HPLC to yield ketopelenolide a (**3**, 0.00027%) and ketopelenolide b (**4**, 0.000093%), respectively. The structures of **2**–**4** were identified by comparison with spectral data in the literature (Fig. 1).[8,9]

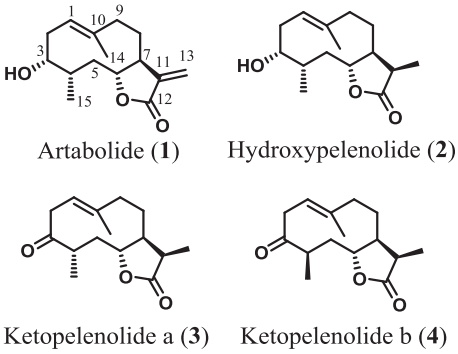

Fig. 1. Structures of isolated compounds **1**–**4**.

2.2. Structural elucidation

The molecular formula of **1** was established as $C_{15}H_{22}O_3$ by high-resolution electrospray ionization mass spectrometry (HR-ESI-MS) [*m*/*z* 273.1493 $(M+Na)^+$, Δ +2.6 mmu], implying a degree of unsaturation of five. The infrared (IR) spectrum exhibited absorption bands at 3447 cm^{-1} for the hydroxyl group and 1751 cm^{-1} for the α,β-unsaturated γ-lactone ring. The ^1H NMR spectrum showed three olefinic protons at δ_H 6.26, 5.56, and 5.55, two of which were doublets assigned to *exo*-olefin protons (δ_H 6.26 and 5.56); two oxymethine protons at δ_H 4.20 and 4.08; two methine protons at δ_H 2.60 and 1.99; six methylene protons at δ_H 2.48, 2.32, 2.31, 2.27, 1.87, and 1.60; a methyl singlet at δ_H 1.73; and a methyl doublet at δ_H 1.03. The ^{13}C NMR spectrum of **1** indicated the presence of 15 carbons, which were assigned to an ester carbonyl carbon at δ_C 170.1; four olefinic carbons at δ_C 140.4, 135.6, 123.9, and 122.2; two oxygenated methine carbons at δ_C 84.9 and 73.0; two methine carbons at δ_C 48.0 and 38.1; four methylene carbons at δ_C 42.0, 40.4, 35.4, and 33.8; and two methyl carbons at δ_C 18.8 and 16.1. Considering that the degree of unsaturation was five, three of these signals could be assigned to two olefins and one carbonyl group. Consequently, **1** was shown to be a bicyclic compound consisting of a 10-membered ring and γ-lactone.

^1H and ^{13}C NMR assignments were supported by 2D NMR ^1H–^1H correlation spectroscopy (COSY), heteronuclear multiple-quantum correlation (HMQC), and heteronuclear multiple bond correlation (HMBC) experiments (Fig. 2). In the 10-membered ring, ^1H–^1H COSY experiments indicated the two substructures by the connectivity of H-1/H-2/H-3 and H-15/H-4/H-5/H-6/H-7/H-8/H-9. The linkages of the two substructures were elucidated by HMBC correlations of H-15/C-3 and H-14/C-1, C-9, and C-10. HMBC experiments suggested the correlations of H-6/C-12, H-13/C-7, C-11, and C-12. Therefore, the connection points between the 10-membered ring and α-methylene-γ-lactone were determined as the C-6 and C-7 positions. Artabolide (**1**) was determined to be a germacranolide-type sesquiterpene lactone, 3-hydroxy-4,6,7(*H*)-germa-cra-1(10),11(13)-dien-6,12-olide.

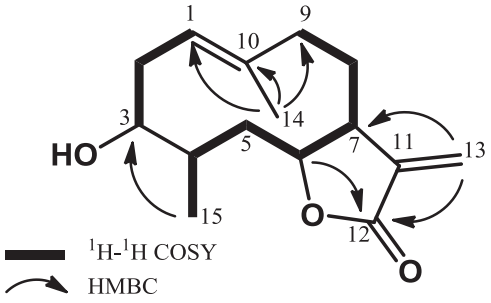

Fig. 2. 2D NMR correlations of **1**.

The relative structure of **1** was deduced from a nuclear Overhauser enhancement spectroscopy (NOESY) spectrum of **1**. The representative correlations are shown in Fig. 3. In the NOESY spectrum, despite the absence of an H-1/H-14 correlation, a correlation of H-2β/H-14 was observed. Thus, the configuration of the C-1/C-10 endocyclic double bond was denoted *E*. Correlations of H-3/H-4 and H-15, H-4/H-6, H-5α/H-7, and H-5β/H-6 and H-15, and the transannular correlations of H-1/H-5α and H-6/H-14 suggested that the relative configuration of **1** was 3*R**, 4*S**, 6*R**, 7*S**.

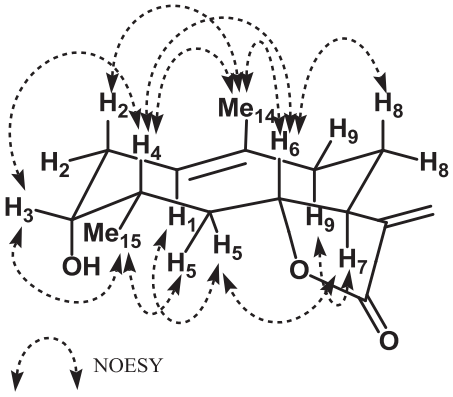

Fig. 3. Representative NOESY correlations of **1**.

To determine the absolute configuration, the modified Mosher's method was applied to **1**.[10] The (*R*)- and (*S*)-MTPA esters (**1a** and **1b**) were prepared by the reaction of **1** with (*S*)- and (*R*)-MTPA chloride, respectively. Each proton signal of **1a** and **1b** was assigned by ^1H–^1H COSY, and $\Delta\delta$ ($\delta_S-\delta_R$) values were obtained (Fig. 4). Judging from the obtained values, the configuration of **1** at C-3 was denoted *R*. Thus, the absolute configuration of **1** was determined to be 3*R*, 4*S*, 6*R*, 7*S*.

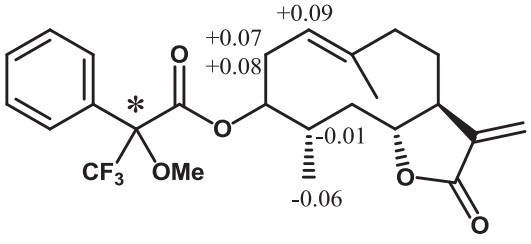

Fig. 4. Representative $\Delta\delta$ values ($\Delta\delta=\delta_S-\delta_R$ in parts per million) obtained from the MTPA esters of **1**.

Artabolide (**1**) was successfully crystallized from an *n*-hexane/EtOAc mixed solution in the orthorhombic space group, $P2_12_12_1$(#19). The ORTEP drawing of **1** is shown in Fig. 5. X-ray crystal structural analysis defined the absolute configuration of **1**, which was in agreement with that described above, and also indicated that the 10-membered ring adopted a chair–chair conformation.

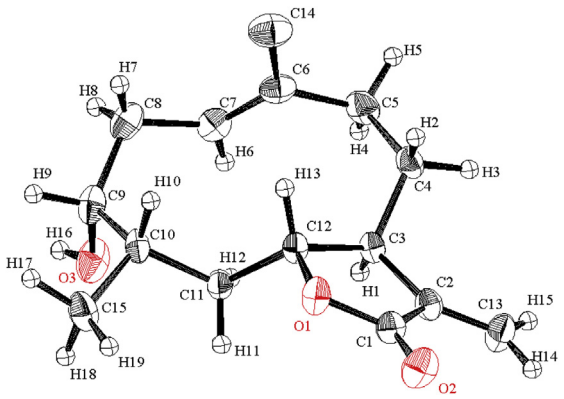

Fig. 5. ORTEP drawing derived from X-ray crystal structural analysis of **1**.

2.3. Inhibitory effects of isolated compounds

The polar auxin transport regulatory activity of isolated compounds **1**–**4** was tested using a suitable radish hypocotyl bioassay system.[11–15] As a result, **1** showed the most potent inhibition of polar auxin transport (Fig. 6). Approximately 2.5 μg/plant treatment of **1** showed ca. 50% inhibition of polar auxin transport compared with that of control. In addition, hydroxypelenolide (**2**) also exhibited the inhibition of polar auxin transport, but the effect was much weaker than that of **1**. Ketopelenolide a (**3**) and ketopelenolide b (**4**) did not show any such activity. These results suggest that the α-methylene-γ-lactone moiety is important for the inhibition of polar auxin transport and that the hydroxyl group of the 10-membered ring may affect the intensity of the activity.

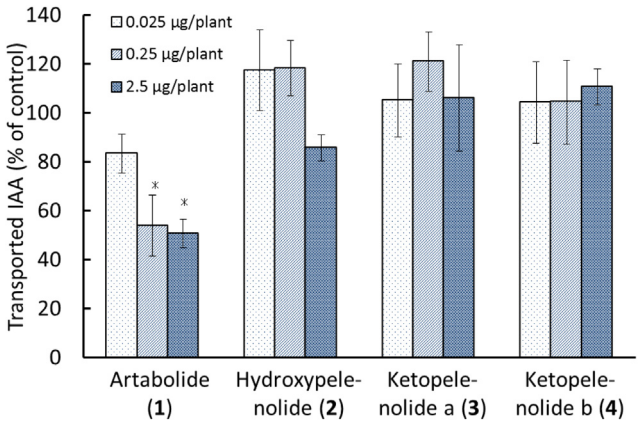

Fig. 6. Polar auxin transport regulation of isolated compounds in radish hypocotyls (*: significant difference, $P<0.01$, $n=4$).

3. Conclusion

A new germacranolide-type sesquiterpene with an α-exo-methylene-γ-lactone moiety, artabolide (**1**), and three known compounds **2**–**4** were isolated from *A. absinthium*. From the results of spectroscopic analysis, the structure of **1** was determined as 3-hydroxy-4,6,7(*H*)-germacra-1(10),11(13)-dien-6,12-olide. The absolute configuration and the spatial conformation of **1** were also determined as *3R*, *4S*, *6R*, *7S*, and chair–chair form by X-ray crystallography and the modified Mosher's method, respectively. By using the radish hypocotyl assay system method, **1** was shown to potently inhibit the polar transport of the plant hormone, IAA, although the other isolated compounds showed weak or no activity. This result indicated that the α-methylene-γ-lactone moiety is important for the inhibition of polar auxin transport. To the best of our knowledge, this is the first report in which a sesquiterpene with an α-methylene-γ-lactone moiety isolated from *A. absinthium* possessed the inhibition of polar auxin transport.

4. Experimental section

4.1. General experimental procedure

Optical rotations were recorded on a JASCO DIP-370 spectrometer. Ultraviolet (UV) spectra were recorded on a HITACHI U-2000A spectrometer. IR spectra were recorded on a JASCO FT/IR-300 spectrometer. ^{1}H and ^{13}C NMR spectra were measured and recorded on a BRUKER Avance 500 spectrometer in $CDCl_3$. The resonances of $CDCl_3$ at δ_H 7.26 and δ_C 77.0 were used as internal references for the ^{1}H and ^{13}C NMR spectra. ESI-MS was recorded on a WATERS SYNAPT G2 mass spectrometer.

4.2. Plant materials

Wormwood (*A. absinthium*) plants were purchased from Keifuen, Chiba, Japan. Radish (*Raphanus sativus* L. var. *longipinnatus* L.H.Bailey cv. shirokukikaiwaredaikon) seeds were purchased from Ishihara Seeds Co. Ltd. Osaka, Japan.

4.3. Extraction and isolation

The aerial parts of *A. absinthium* (750 gFW) were finely cut and extracted with 80% acetone/H_2O (3 L) three times at 6 °C for 7 days. After filtration, the acetone extract was evaporated in a rotary evaporator. The residue (33.6 g) was partitioned between EtOAc (400 mL×3) and H_2O (400 mL). The EtOAc-soluble portion (8.19 g) was subjected to a silica-gel column chromatography (ϕ 4.6×36 cm) with *n*-hexane/EtOAc (90:10→80:20→70:30→60:40→50:50→30:70→0:100) stepwise gradient and separated into 12 fractions (AAEA1-12). AAEA8 (231 mg) was rechromatographed on a silica-gel column (ϕ 1.1×36 cm) with toluene/EtOAc (98:2→90:10→80:20→70:30→60:40→50:50→0:100) to afford 11 fractions (AAEA8-1-8-11). AAEA8-5 (68.0 mg) was subjected to separation on a Sep-Pak ODS cartridge (Waters) with MeOH/H_2O (20:80→40:60→60:40→80:20→100:0) to afford a mixture of compounds **1** and **2**. The mixture (29.0 mg) was purified by reversed-phase HPLC (TSK-gel ODS-120A, TOSOH, ϕ 7.8×300 mm, flow rate 1.5 mL/min, 55%MeOH isocratic) to yield artabolide (**1**, 1.9 mg) and hydroxypelenolide (**2**, 16.3 mg). AAEA6 (165 mg) was subjected to separation on a Sep-Pak ODS cartridge (Waters) with MeOH/H_2O (50:50→60:40→70:30→80:20→90:10→100:0) and $CHCl_3$/MeOH (50:50→100:0) to afford eight fractions (AAEA6-1-6-8). AAEA 6-2 (13.1 mg) was purified by reversed-phase HPLC (TSK-gel ODS-120A, TOSOH, ϕ 7.8×300 mm, flow rate 2.0 mL/min, 60% MeCN isocratic) to yield ketopelenolide a (**3**, 2.0 mg). AAEA8-2 (5.9 mg) was also purified by reversed-phase HPLC (TSK-gel ODS-120A, TOSOH, ϕ 7.8×300 mm, flow rate 2.0 mL/min, 55%MeOH isocratic) to yield ketopelenolide b (**4**, 0.7 mg).

*4.3.1. Artabolide (**1**).* Colorless prism; $[\alpha]_D^{24}$ −27.2 (*c* 1.00, $CHCl_3$); IR (KBr) ν_{max} 3447 and 1751 cm^{-1}; UV λ_{max} (MeOH) nm (log ε) 206 (4.0); ^1H (500 MHz, $CDCl_3$) and ^{13}C NMR (125 MHz, $CDCl_3$) data are given in Table 1; ESI-MS (positive ion) *m*/*z* 273 $(M+Na)^+$, HR-ESI-MS *m*/*z* 273.1493 (calcd for $C_{15}H_{22}O_3Na$: 273.1467).

Table 1
^1H, ^{13}C NMR, and NOESY spectral data of artabolide (**1**)

Position	δ_H (mult., *J* in Hz)	δ_C	NOESY
1	5.55 (m)	123.9	H-2α, H-2β, H-5α, H-9α, H-9β
2α	2.48 (ddd, 14.0, 10.3, 3.5)	33.8	H-1, H-3, H-14
2β	2.27 (overlapped)		H-1, H-3, H-4, H-6, H-14
3	4.08 (m)	73.0	H-2α, H-2β, H-4, H-15
4	1.99 (m)	38.1	H-2β, H-3, H-5α, H-6, H-15
5α	2.31 (overlapped)	42.0	H-1, H-4, H-6, H-7
5β	1.60 (overlapped)		H-6, H-15
6	4.20 (dd, 7.4, 4.6)	84.9	H-2β, H-4, H-5α, H-5β, H-7, [a]H-8α, H-8β, H-14
7	2.60 (m)	48.0	H-5α, H-6,[a] H-8α, H-8β, H-9α, H-13b
8α	1.87 (m)	35.4	H-6, H-7, H-9α, H-9β
8β	1.87 (m)		H-6, H-7, H-9α, H-9β
9α	2.32 (overlapped)	40.4	H-1, H-7, H-8α, H-8β
9β	2.32 (overlapped)		H-1, H-8α, H-8β, H-14
10	—	135.6	
11	—	140.4	
12	—	170.1	
13a	6.26(d, 2.9)	122.2	
13b	5.56(d, 2.9)		H-7
14	1.73(s)	16.1	H-2α, H-2β, H-6, H-9β
15	1.03(d, 7.0)	18.8	H-3, H-4, H-5β

[a] Weak correlation.

4.4. Preparation of MTPA esters of artabolide (1)

(−)-(*R*)-MTPACl (2.1 μL, 4 equiv) and DMAP (0.5 mg) were added to a solution of artabolide (**1**, 0.7 mg) in anhydrous CH_2Cl_2 (100 μL). After stirring at room temperature for 2.5 h, the reaction mixture was concentrated under nitrogen gas. The residue was applied to a silica-gel column (ϕ 0.1×10 cm, *n*-hexane:EtOAc=9:1) to yield (*S*)-MTPA ester (**1a**, 0.6 mg). (+)-(*S*)-MTPACl (1.8 μL, 4 equiv) and DMAP (0.5 mg) were added to a solution of artabolide (**1**, 0.6 mg) in anhydrous CH_2Cl_2 (100 μL). After stirring at room temperature for 2.5 h, the reaction mixture was concentrated under nitrogen gas. The residue was applied to a silica-gel column (ϕ 0.1×10 cm, *n*-hexane:EtOAc=9:1) to yield (*R*)-MTPA ester (**1b**, 0.5 mg).

*4.4.1. Artabolide-(S)-MTPA ester (**1a**).* ^1H NMR (500 MHz, $CDCl_3$) δ 7.53–7.45 (5H, phenyl protons); 6.28 (1H, d, *J*=3.0 Hz, H-13a); 5.59 (1H, d, *J*=2.6 Hz, H-13b); 5.39 (1H, overlapped, H-1); 5.38 (1H, overlapped, H-3); 4.20 (1H, br s, H-6); 3.56 (3H, s, −OMe); 2.63 (1H, m, H-2α); 2.57 (1H, br s, H-7); 2.40 (1H, m, H-2β); 2.36 and 2.25 (2H, overlapped, H-9); 2.01 (1H, overlapped, H-4); 1.91 (2H, overlapped, H-8); 1.83 (3H, overlapped, H-14); 1.25 (2H, overlapped, H-5); 0.94 (3H, d, *J*=6.7 Hz, H-15); ESI-MS (positive ion) *m*/*z* 489 $(M+Na)^+$, HR-ESI-MS *m*/*z* 489.1862 (calcd for $C_{25}H_{29}O_5F_3Na$: 489.1865).

*4.4.2. Artabolide-(R)-MTPA ester (**1b**).* ^1H NMR (500 MHz, $CDCl_3$) δ 7.56–7.45 (5H, phenyl protons); 6.28 (1H, d, *J*=2.9 Hz, H-13a); 5.59 (1H, d, *J*=2.5 Hz, H-13b); 5.35 (1H, overlapped, H-3); 5.30 (1H, overlapped, H-1); 4.20 (1H, br s, H-6); 3.54 (3H, s, −OMe); 2.56 (1H, overlapped, H-2α); 2.56 (1H, overlapped, H-7); 2.32 (1H, overlapped, H-2β); 2.35 and 2.23 (2H, overlapped, H-9); 2.01 (1H, br s, H-4); 1.91 (2H, overlapped, H-8); 1.83 (3H, overlapped, H-14); 1.27 (2H, overlapped, H-5); 1.00 (3H, d, *J*=6.7 Hz, H-15); ESI-MS (positive ion) *m*/*z* 489 $(M+Na)^+$, HR-ESI-MS *m*/*z* 489.1862 (calcd for $C_{25}H_{29}O_5F_3Na$: 489.1865).

4.5. X-ray crystal structure analysis

A colorless prism crystal of **1** having approximate dimensions of 0.200×0.200×0.200 mm was mounted on a glass fiber. X-ray crystal structure analysis was conducted on a Rigaku R-AXIS RAPID diffractometer with graphite monochromated Cu-Kα radiation. The crystal-to-detector distance was 127.40 mm. Cell constants and an orientation matrix for data collection corresponded to a primitive orthorhombic cell with dimensions: *a*=7.7594(2) Å, *b*=10.0447(2) Å, *c*=17.4056(4) Å, *V*=1356.60(5) $Å^3$. For *Z*=4 and F.W.=250.34, the calculated density was 1.226 g/cm^3. The reflection conditions of: *h*00: *h*=2*n*, 0*k*0: *k*=2*n*, 00*l*: *l*=2*n*, uniquely determine the space group to be: $P2_12_12_1$ (#19).

Of the 14,859 reflections that were collected, 2465 were unique (R_{int}=0.0335). The linear absorption coefficient, μ, for Cu-Kα radiation was 6.723 cm^{-1}. The data were corrected for Lorentz and polarization effects. The structure was solved by direct methods and expanded using Fourier techniques. The non-hydrogen atoms were refined anisotropically. Hydrogen atoms were refined isotropically. The final cycle of full-matrix least-squares refinement on F2 was based on 2465 observed reflections and 240 variable parameters and converged (largest parameter shift was 0.00 times its esd) with unweighted and weighted agreement factors of: *R*1=0.0398, *wR*2=0.1158. All calculations were performed using the Crystal Structure crystallographic software package except for refinement, which was performed using SHELXL-97 software. Crystallographic data for **1** have been deposited with the Cambridge Crystallographic Data Center (deposit No. CCDC 923140). Copies of the data can be obtained, free of change, on application to the Director, CCDC, 12 Union Road, Cambridge CB2, 1EZ, U.K. (e-mail: deposit@ccdc.cam.ac.uk).

4.6. Bioassay for polar auxin transport

Measurement of polar auxin transport was performed according to the method previously reported with suitable modification.[11–15] Briefly, 2-cm hypocotyl segments were excised from 6-day-old radish seedlings and charged into 1.5-mL Eppendorf plastic tubes in inverted orientation. Twenty microliters of 1% agar containing ^{14}C-labeled IAA (American Radiolabeled Chemicals, Inc., St. Louis, MO, USA.) with or without the test compound was supplied at the bottom of the tubes. After incubation at room temperature for 9–18 h, a 2-mm piece of the opposite side of the segment was cut and directly put into a vial of liquid scintillation cocktails. Radioactivity of the small slices was counted by a liquid scintillation counter.

Acknowledgements

This study was partially supported by a Grant-in-Aid for Scientific Research on Innovative Areas 'Chemical Biology of Natural Products' (Grant No. 24102509) from The Ministry of Education, Culture, Sports, Science and Technology, Japan.

References and notes

1. Marchant, A.; Kargul, J.; May, S. T.; Muller, P.; Delbarre, A.; Perrot-Rechenmann, C.; Bennett, M. J. *EMBO J.* **1999**, *18*, 2066–2073.
2. Gälweiler, L.; Guan, C.; Müller, A.; Wisman, E.; Mendgen, K.; Yephremov, A.; Palme, K. *Science* **1998**, *282*, 2226–2230.
3. Sidler, M.; Hassa, P.; Hasan, S.; Ringli, C.; Dudler, R. *Plant Cell* **1998**, *10*, 1623–1636.
4. Blakeslee, J. J.; Bandyopadhyay, A.; Lee, O. R.; Mravec, J.; Titapiwatanakun, B.; Sauer, M.; Makam, S. N.; Cheng, Y.; Bouchard, R.; Adamec, J.; Geisler, M.;

Nagashima, A.; Sakai, T.; Martinoia, E.; Friml, J.; Peer, W. A.; Murphy, A. S. *Plant Cell* **2007**, *19*, 131–147.
5. Jacobs, M.; Rubery, P. H. *Science* **1988**, *241*, 346–349.
6. Brown, D. E.; Rashotte, A. M.; Murphy, A. S.; Normanly, J.; Tague, B. W.; Peer, W. A.; Taiz, L.; Muday, G. K. *Plant Physiol.* **2001**, *126*, 524–535.
7. Ueda, J.; Toda, Y.; Kato, K.; Kuroda, Y.; Arai, T.; Hasegawa, T.; Shigemori, H.; Hasegawa, K.; Kitagawa, J.; Miyamoto, K.; Uheda, E. *Acta Physiol. Plant.* **2013**, http://dx.doi.org/10.1007/s11738-013-1261-6
8. Suchý, M.; Samek, Z.; Herout, V.; Bates, R. B.; Snatzke, G.; Šoam, F. *Collect. Czech. Chem. Commun.* **1967**, *32*, 3917–3925.
9. Wang, W. Z.; Tan, R. X.; Yao, Y. M.; Wang, Q.; Jiang, F. X. *Phytochemistry* **1994**, *37*, 1347–1349.
10. Ohtani, I.; Kusumi, T.; Kashman, Y.; Kakisawa, H. *J. Org. Chem.* **1991**, *56*, 1296–1298.
11. Oka, M.; Ueda, J.; Miyamoto, K.; Yamamoto, R.; Hoson, T.; Kamisaka, S. *Biol. Sci. Space* **1995**, *9*, 331–336.
12. Oka, M.; Miyamoto, K.; Okada, K.; Ueda, J. *Plant Cell Physiol.* **1999**, *40*, 231–237.
13. Okada, K.; Ueda, J.; Komaki, M. K.; Bell, C. J.; Shimura, Y. *Plant Cell* **1991**, *3*, 677–684.
14. Ueda, J.; Miyamoto, K.; Yuda, T.; Hoshino, T.; Fujii, S.; Mukai, C.; Kamigaichi, S.; Aizawa, S.; Yoshizaki, I.; Shimazu, T.; Fukui, K. *J. Plant Res.* **1999**, *112*, 487–492.
15. Ueda, J.; Miyamoto, K.; Yuda, T.; Hoshino, T.; Fujii, S.; Mukai, C.; Kamigaichi, S.; Aizawa, S.; Yoshizaki, I.; Shimazu, T.; Fukui, K. *Biol. Sci. Space* **2000**, *14*, 47–57.